# Numerical Simulation of Three-dimensional Breaking Waves and its Interaction with a Cylinder

**Z. Xie[1,2,3], L. Lu[3], T. Stoesser[1], J. Lin[4], D. Pavlidis[2], P. Salinas[2], C. C. Pain[2], O. K. Matar[2]**

[1]School of Engineering, Cardiff University, Cardiff, CF 24 3AA, U.K.
[2]Department of Chemical Engineering, Imperial College London, London, SW7 2AZ, U.K.
[3]State Key Laboratory of Coastal and Offshore Engineering, Dalian University of Technology, Dalian 116024, China.
[4]College of Environmental Science and Engineering, Dalian Maritime University, Dalian 116026, China.
Email: zxie@cardiff.ac.uk

## 1 Introduction

Wave breaking plays an important role in marine hydrodynamics, wave-structure interaction, air-sea interaction, surf zone dynamics, and nearshore sediment transport, Several three-dimensional (3D) two-phase flow models have been developed to study 3D breaking waves in a periodic space domain (Lubin *et al.*, 2006), over a plane beach (Lakehal & Liovic, 2011) and over a complex topography (Xie, 2015), which have provided much insight into the kinematics and dynamics of breaking waves, including the overturning jet and the subsequent splash-up process. Previous investigations have greatly improved our knowledge of breaking waves, However, little attention has been given for the numerical study on the 3D wave-structure interaction over a slope. In this study, a 3D two-phase flow model with adaptive unstructured meshes is developed to investigate 3D breaking wave interaction with a vertical cylinder along a constant sloping beach, which can provide detailed information on the impact force and energy dissipation during wave breaking.

## 2 Mathematical Model

A multi-fluid modelling framework has been developed based on the multi-component modelling approach with information on interfaces embedded into the continuity equations. In two-phase flows, let $\alpha_i$ be the mass fraction of phase $i$, where $i = 1, 2$, the density and dynamic viscosity of phase $i$ are $\rho_i$ and $\mu_i$, respectively. A constraint on the system is:

$$\sum_{i=1}^{2} \alpha_i = 1. \quad (1)$$

For each fluid component $i$, the conservation of mass may be defined as,

$$\frac{\partial}{\partial t}(\alpha_i) + \nabla \cdot (\alpha_i \mathbf{u}) = 0, \quad i = 1, 2, \quad (2)$$

and the equations of motion of an incompressible fluid may be written as:

$$\frac{\partial(\rho \mathbf{u})}{\partial t} + \nabla \cdot (\rho \mathbf{u} \otimes \mathbf{u}) = -\nabla p + \nabla \cdot [\mu(\nabla \mathbf{u} + \nabla^{\mathrm{T}} \mathbf{u})] + \rho \mathbf{g} + \sigma \kappa \mathbf{n} \delta, \tag{3}$$

where $t$ is the time, $\mathbf{u}$ is velocity vector, $p$ is the pressure, the bulk density is $\rho = \sum_{i=1}^{2} \alpha_i \rho_i$, the bulk dynamic viscosity is $\mu = \sum_{i=1}^{2} \alpha_i \mu_i$, $\mathbf{g}$ is the gravitational acceleration vector, $\sigma$ is the surface tension coefficient, $\kappa = \nabla \cdot \mathbf{n}$ is the interfacial curvature, $\mathbf{n}$ is the interface unit normal, and $\delta$ is the Dirac delta function.

# 3 Numerical Method

In the present study, a transient, mixed, control-volume and finite-element formulation is used to discretise the governing equations (Equation 2 and Equation 3). A finite volume discretisation of the continuity equations and a linear discontinuous Galerkin (DG) (Pavlidis *et al.*, 2016) discretisation of the momentum equations are employed with backward Euler time stepping. Within each time-step, the equations are iterated upon using a projection-based pressure determination method until all equations are simultaneously balanced. The main numerical framework includes a finite element type ($\mathrm{P_1DG\text{-}P_2}$) for multi-fluid flow problems, which ensures exact balance between buoyancy force and pressure gradient. The framework also features a novel interface capturing scheme based on compressive control volume advection method (Pavlidis *et al.*, 2016), involving a high-order accurate finite element method to obtain fluxes on the control volume boundaries, where these fluxes are subject to flux-limiting using a normalised variable diagram approach to obtain bounded and compressive solutions for the interface. The implementation of capillary/surface tension force in the framework using an unstructured mesh minimises spurious velocities often found in interfacial flows (Xie *et al.*, 2016). Finally, use of anisotropic unstructured mesh adaptivity (Pain *et al.*, 2001) allows the grid resolution to be concentrated in relatively important regions, such as the vicinity of interfaces, while lower resolution can be used in other regions; this leads to a significant gain in computational efficiency without sacrificing accuracy.

# 4 Results and Discussion

A three-dimensional solitary breaking wave over a constant slope is investigated here. In the computation, the origin of the coordinates is located at the still water level in the centre of the toe of the slope and all lengths are normalized by the water depth $D = 0.3048$ m. The compuational setup is similiar to the case for a 3D breaking wave without a cylinder in Xie (2015), in which the slope is 1:15 and the incident plane solitary wave with the ratio of wave height to water depth is $H/D = 0.45$. A vertical cylinder with a diameter of $d/D = 0.33$ is considered here and it is located at a distance of $x = 12.5D$ from the toe of the slope. The computational domain, which has a length of $19.75D$, width of $1.3D$, and height of $1.75D$, is discretized by an adaptive fully-unstructured mesh, with minimum meshes of $\Delta x_{\mathrm{min}}/D = 0.02$, $\Delta y_{\mathrm{min}}/D = 0.02$ and $\Delta z_{\mathrm{min}}/D = 0.05$ in the steamwise, vertical and spanwise directions, respectively.

Figure 1 shows snapshots of detailed views of the solitary wave before, during and after wave breaking. Before wave breaking, it can be seen that the wave crest becomes steep due to the shoaling effect (figure 1(a)). A typical three-dimensional overturning jet just ahead of the cylinder can be seen in figure 1(b) during wave breaking. The breaking wave impacts with

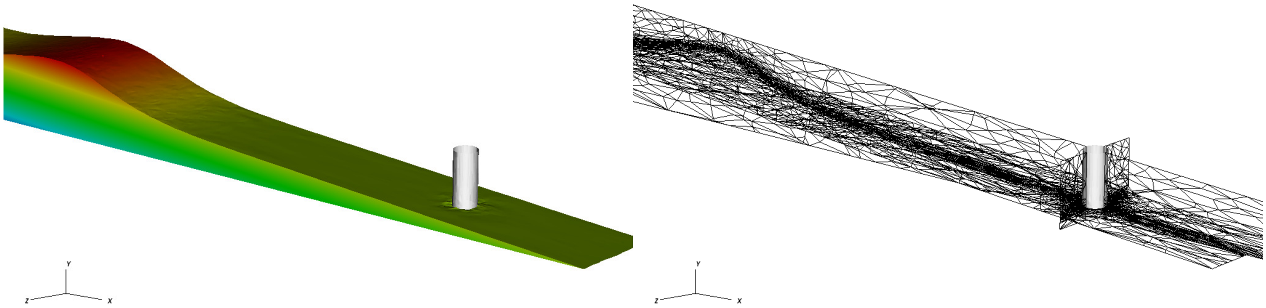

(a) before wave breaking

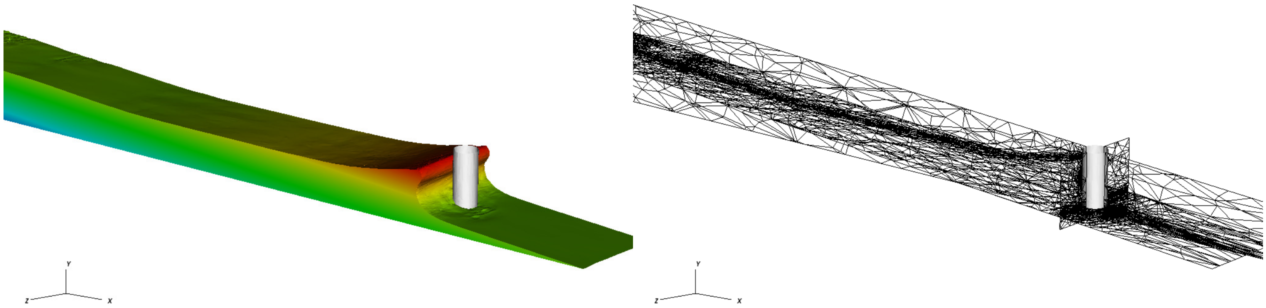

(b) during wave breaking

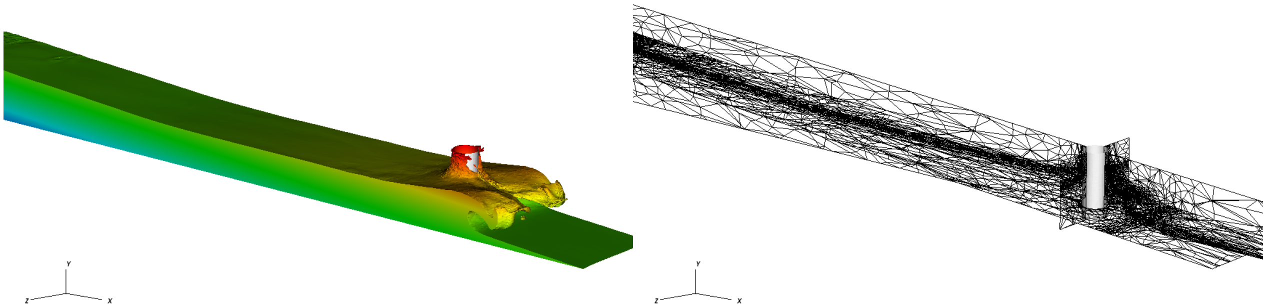

(c) after wave breaking

Figure 1: Detailed views of the water wave surface before (a), during (b) and after (c) wave breaking. Left pannel shows the water surfaces colored based on local values of $y/D$ and right pannel shows the fully-unstructured mesh corresponded to the left pannel along three slices.

the vertical cylinder and 3D complex plunging jet is developed in figure 1(c). The adaptive fully-unstructured meshes are also shown in figure 1 and it can be seen that finer mesh is used in the vicinity of the interface and the region near the cylinder whereas coarser mesh is used away from the interface. This has the advantage of reducing computational effort without sacrificing accuracy. More detailed results of the kinematics and dynamics of 3D breaking waves interaction with the vertical cylinder will be presented at the workshop.


## Acknowledgements

The first and second authors would like to acknowledge the financial support by the Open Awards of the State Key Laboratory of Coastal and Offshore Engineering at Dalian University of Technology and this work was also funded by the EPSRC MEMPHIS multiphase Programme Grant (number EP/K003976/1).


## References


Lakehal, D. & Liovic, P 2011 Turbulence structure and interaction with steep breaking waves. *Journal of Fluid Mechanics* **674**, 522–577.

Lubin, P., Vincent, S., Abadie, S. & Caltagirone, J. P. 2006 Three-dimensional large eddy simulation of air entrainment under plunging breaking waves. *Coastal Engineering* **53** (8), 631–655.

Pain, C. C., Umpleby, A. P., de Oliveira, C. R. E. & Goddard, A. J. H. 2001 Tetrahedral mesh optimisation and adaptivity for steady-state and transient finite element calculations. *Computer Methods in Applied Mechanics and Engineering* **190**, 3771–3796.

Pavlidis, D., Gomes, J. L. M. A., Xie, Z., Percival, J. R., Pain, C. C. & Matar, O. K. 2016 Compressive advection and multi-component methods for interface-capturing. *International Journal of Numerical Methods in Fluids* **80**, 256–282.

Xie, Z. 2015 A two-phase flow model for three-dimensional breaking waves over complex topography. *Proceedings of the Royal Society A: Mathematical, Physical & Engineering Sciences* **471**, 20150101.

Xie, Z., Pavlidis, D., Salinas, P., Percival, J. R., Pain, C. C. & Matar, O. K. 2016 A balanced-force control volume finite element method for interfacial flows with surface tension using adaptive anisotropic unstructured meshes. *Computers and Fluids* **138**, 38–50.